REPORT DOCUMENTATION PAGE

Form Approved
OMB No. 0704-01-0188

PLEASE DO NOT RETURN YOUR FORM TO THE ABOVE ADDRESS.

1. REPORT DATE *(DD-MM-YYYY)*	2. REPORT TYPE	3. DATES COVERED *(From - To)*
05–2002	Technical	

4. TITLE AND SUBTITLE

TRACKING PERFORMANCE OF THE RLS ALGORITHM APPLIED TO AN ANTENNA ARRAY IN A REALISTIC FADING ENVIRONMENT

5a. CONTRACT NUMBER

5b. GRANT NUMBER

5c. PROGRAM ELEMENT NUMBER
0601152N

6. AUTHORS

B. C. Banister
UCSD

J. R. Zeidler
SSC San Diego

5d. PROJECT NUMBER

5e. TASK NUMBER

5f. WORK UNIT NUMBER

7. PERFORMING ORGANIZATION NAME(S) AND ADDRESS(ES)

SSC San Diego
San Diego, CA 92152-5001

8. PERFORMING ORGANIZATION REPORT NUMBER

9. SPONSORING/MONITORING AGENCY NAME(S) AND ADDRESS(ES)

Office of Naval Research
800 North Quincy Street
Arlington, VA 22217–5000

10. SPONSOR/MONITOR'S ACRONYM(S)

11. SPONSOR/MONITOR'S REPORT NUMBER(S)

12. DISTRIBUTION/AVAILABILITY STATEMENT

Approved for public release; distribution is unlimited.

13. SUPPLEMENTARY NOTES

14. ABSTRACT

In this paper, frequency domain techniques are used to derive the tracking properties of the recursive least squares (RLS) algorithm applied to an adaptive antenna array in a mobile fading environment, expanding the use of such frequency domain approaches for nonstationary RLS tracking to the interference canceling problem that characterizes the use of antenna arrays in mobile wireless communications. The analysis focuses on the effect of the exponential weighting of the correlation estimation filter and its effect on the estimation of the time variant autocorrelation matrix and cross-correlation vector. Specifically, the case of a flat Rayleigh fading desired signal applied to an array in the presence of static interferers is considered with an AR2 fading process approximating the Jakes' fading model. The result is a mean square error (MSE) performance metric parameterized by the fading bandwidth and the RLS exponential weighting factor, allowing optimal parameter selection. The analytic results are verified and demonstrated with a simulation example.

Published in *IEEE Transactions on Signal Processing,* vol. 50, no. 5, 1037–1050.

15. SUBJECT TERMS

Mission Area: Surveillance

antenna array; fading; multipath; recursive least squares; spectral analysis

16. SECURITY CLASSIFICATION OF:			17. LIMITATION OF ABSTRACT	18. NUMBER OF PAGES	19a. NAME OF RESPONSIBLE PERSON
a. REPORT	b. ABSTRACT	c. THIS PAGE			J. R. Zeidler
U	U	U	UU	14	19B. TELEPHONE NUMBER *(Include area code)* (619) 553-1581

Tracking Performance of the RLS Algorithm Applied to an Antenna Array in a Realistic Fading Environment

Brian C. Banister and James R. Zeidler, *Fellow, IEEE*

***Abstract*—In this paper, frequency domain techniques are used to derive the tracking properties of the recursive least squares (RLS) algorithm applied to an adaptive antenna array in a mobile fading environment, expanding the use of such frequency domain approaches for nonstationary RLS tracking to the interference canceling problem that characterizes the use of antenna arrays in mobile wireless communications. The analysis focuses on the effect of the exponential weighting of the correlation estimation filter and its effect on the estimations of the time variant autocorrelation matrix and cross-correlation vector. Specifically, the case of a flat Rayleigh fading desired signal applied to an array in the presence of static interferers is considered with an AR2 fading process approximating the Jakes' fading model. The result is a mean square error (MSE) performance metric parameterized by the fading bandwidth and the RLS exponential weighting factor, allowing optimal parameter selection. The analytic results are verified and demonstrated with a simulation example.**

***Index Terms*—Antenna array, fading, multipath, recursive least squares, RLS, spectral analysis.**

I. Introduction

THE use of mobile wireless systems has been growing rapidly, and with this growth has come the need for greater network capacity and a corresponding increase in the sophistication of the communication systems themselves. An important area for the enhancement of network capacity is the use of antenna arrays, which can provide performance enhancement through both interference suppression and spatial fading diversity [1], [2]. The mobile wireless channel provides special difficulties for receive array algorithm design, giving rise to fast fading channels that must be accurately estimated and tracked for coherent modulation systems. This paper analyzes the tracking performance of such an antenna array when recursive least squares (RLS) is used to generate the combining weights.

Manuscript received April 21, 2000; revised January 24, 2002. This work was supported in part by CoRe research Grant core00-10074. The associate editor coordinating the review of this paper and approving it for publication was Prof. S. M. Jesus.

B. C. Banister is with the Department of Electrical and Computer Engineering, University of California at San Diego, La Jolla, CA 92093 USA, and also with LSI Logic Corporation, San Diego CA 92121-1002 USA (e-mail: banister@ece.ucsd.edu).

J. R. Zeidler is with the Department of Electrical and Computer Engineering, University of California at San Diego, La Jolla, CA 92093 USA, and also with Space and Naval Warfare Systems Center, San Diego, CA 92170 USA (e-mail: zeidler@nosc.mil).

Publisher Item Identifier S 1053-587X(02)03280-4.

Due to their relative simplicity, algorithms employing weighted linear combining of the signals from each antenna are most commonly considered, and many such algorithms exist [3]. Wiener combining techniques, which were originally applied to the antenna problem by Widrow *et al.* in [4], provide the linear output estimate of the desired signal with minimum mean square error (MMSE). Wiener combining can be considered optimal in the additional sense of providing the *maximum a posteriori* (MAP) signal estimate in the presence of Gaussian noise and interference [5], which is commonly applied to the decoding of received signals [2]. Previous results on the performance of Wiener algorithms applied to antenna arrays have derived the average signal-to-interference ratio [6] and outage probabilities [7] for array systems with perfect tracking in a fading environment. Metrics such as mean squared error (MSE) and bit error rate (BER) for receive antenna arrays in a fading environment have been found by simulation [8]–[10]. This paper goes further in that it provides analytic results for the tracking performance of RLS in such an environment, allowing optimization of performance in the Rayleigh fading channel.

RLS [11], typically exponentially weighted (EW-RLS), is a commonly considered adaptive Wiener technique. Tracking of adaptive prediction with RLS has been analyzed for zero bandwidth [12] and finite bandwidth [13] chirped signals. Optimization of the windowing function for prediction of a chirped signal is considered in [14]. Tracking in system identification problems has been studied in [15]–[18] for a first-order Markov process. These previous results consider the performance of RLS for prediction and identification problems in nonstationary environments with simple models defined by a single parameter and a static or deterministically time-variant receive vector autocorrelation matrix. These models do not apply to the interference canceling problem characterizing a receive antenna array in communications, and such closed-form tracking analyses cannot be found for the interference canceling problem.

Spectral techniques have been applied to RLS tracking analysis of system identification applications in [19] and [20]. An important advance to the analysis of RLS tracking in [19] is the derivation of the MSE for a general class of signals in terms of the power spectral density (PSD) of the nonstationarity. In addition to deriving the MSE performance of EW-RLS, [19] shows that weighting functions other than the exponential weighting give better performance and derives the optimal weighting as a function of the PSDs of the nonstationary process and the noise.

This paper derives the MSE at the output of an RLS combiner for an antenna array operating with a model of a dynamic fading

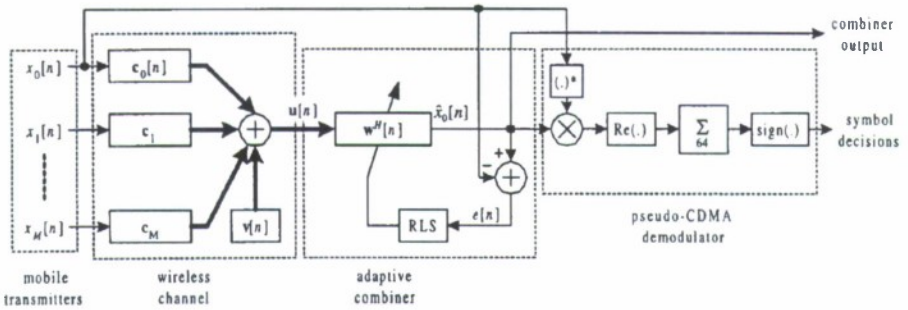

Fig. 1. Block diagram of the adaptive combiner with crossover detector modeling bit decisions for BER simulations.

channel appropriate to mobile wireless communications problems. The system block diagram is shown in Fig. 1. Similar to [19], spectral analysis tools are applied to the analysis problem. However, it is found that the array problem introduces an additional hurdle to the analysis. In the system presented in [19], the autocorrelation matrix of the received vector is time invariant, whereas in the array problem, this matrix is time variant, and the resulting effects must be carefully considered. A new technique of quasideterministic approximation of the least square (LS) sample correlation matrix that captures its relationship with the sample cross-correlation vector is introduced. It is found that the effects of the LS weighting function and fading PSD can be separated from the statistical expectations, providing a tractable analytic solution. The results allow for the selection of the optimal exponential "forgetting" factor for EW-RLS.

In the interest of tractability, the channel model has been simplified to a level that allows demonstration of the relevant performance measures. Signals are represented in discrete time. All impinging signals are considered to be planewaves from the far-field, and the modulation is considered to be "narrowband" in the sense that the time delay across the array can be modeled as a carrier phase shift. The desired signal is degraded by flat Rayleigh fading with an approximate Jakes Doppler spectrum defining the fading process, whereas the interfering signal channels are static. While the system under study is assumed to be DS-CDMA, issues of code phase tracking and resolvable multipath are ignored in favor of clearly demonstrating the channel-tracking properties of the RLS algorithm. It is worth noting, however, that the RLS algorithm would, in practice, have to be applied independently to each of several resolvable multipath signals in a DS-CDMA system. Thus, the analysis here presented would apply equally to each such path.

II. Preliminaries

A. Vector Signal Models for a Signal and Interference

An overview of models that have been considered for use with antenna arrays is presented in [21]. This study uses the simplest possible fading model and neglects issues of time and angular dispersion in order to focus on the performance of the adaptive tracking. The channel model corresponds to that shown in Fig. 2, where the desired mobile experiences local multipath reflections. The angular dispersion φ of the desired mobile's signal as received by the base station is small; therefore, the fades experienced by the multiple antennas are identical. This channel

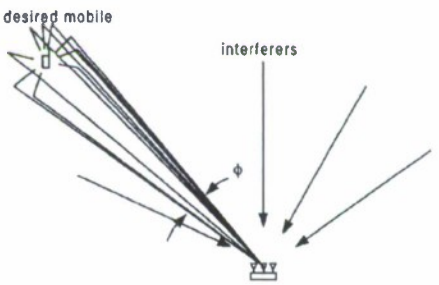

Fig. 2. Environmental conditions modeled in the analysis.

model allows for performance enhancement from the array due to beam steering and null forming but not from receive diversity. Similarly, the time dispersion is small so that multipath is not resolvable in the receiver. If the local scatters are uniformly distributed around the mobile, then the fading envelope has a correlation defined by the Jakes' model [22].

There are $M+1$ users, with baseband signals represented by the $(M+1)\times 1$ vector $\mathbf{x}[n]$. These modulation streams are assumed to have constant unit power, to be independent from each other, and to be uncorrelated from time sample to time sample so that

$$E(\mathbf{x}[n]\mathbf{x}^H[n-m] = \mathbf{I}\delta[m]) \tag{1}$$

where $\delta[m]$ is the Kronecker delta function. This signal model may represent DS-CDMA sampled at the chip rate or a narrow band system sampled at the symbol rate.

$x_0[n]$ is the signal of the desired transmitter. It is convenient at several points to consider the aggregated interferers, and a tilde is used throughout for this purpose so that

$$\tilde{\mathbf{x}}[n] = [x_1[n] \quad x_2[n] \quad \dots \quad x_M[n]]^T. \tag{2}$$

The signal received by the N antennas is a linear combination of the signals from the $M+1$ users, as determined by the time-varying channel matrix $\mathbf{C}[n]$, plus a white noise term $\mathbf{v}[n]$.

$$\mathbf{u}[n] = \mathbf{C}[n]\mathbf{x}[n] + \mathbf{v}[n]. \tag{3}$$

The channel matrix is comprised of the response of the desired signal and of the interferers, giving

$$\mathbf{C}[n] = [\mathbf{c}_0[n] \quad \tilde{\mathbf{C}}]. \tag{4}$$

The white noise term has an autocorrelation given by

$$E(\mathbf{v}[n]\mathbf{v}^H[n-m]) = \sigma_v^2 \mathbf{I}\delta[m]. \tag{5}$$

For an array operating on signals from point sources in the far field, the channel matrix can be given as

$$\mathbf{C}[n] = \mathbf{D}\mathbf{A}[n] \tag{6}$$

where $\mathbf{D}$ is the matrix comprised of the uniform linear array (ULA) steering vectors [21] of the $M+1$ users and N antennas, and $\mathbf{A}[n]$ is the time-varying diagonal matrix giving the time-varying complex channel gains for each user. We then have (7), shown at the bottom of the page, and

$$\mathbf{A}[n] = \begin{bmatrix} \alpha_0[n] & & & \\ & \alpha_1 & & \\ & & \cdots & \\ & & & \alpha_M \end{bmatrix} \tag{8}$$

$$\sigma_0^2 = E(|\alpha_0[n]|^2) \tag{9}$$

where $\alpha_0[n]$ is the complex channel gain of the Rayleigh fading desired signal, and α_i for $i \neq 0$ is a constant channel gain associated with each of the interferers. The use of constant channel gains for each interferer contributes to the tractability of the analysis since the value of γ, which was introduced in (78), is constant. For a number of interferers significantly larger than the number of antennas, one would expect that the results with constant gains would approximate the result with fading interferers. Δ is the wavelength normalized linear antenna spacing for a carrier frequency ω, and θ_i is the angle of arrival of the ith signal.

$$\Delta = \frac{\omega}{2\pi \cdot (\text{speed of light})} \cdot (\text{antenna spacing distance.})$$

For simplicity of notation, $E_C(\cdot) \Leftrightarrow E(\cdot \mid \mathbf{C}[n])$ will denote expectation given the random channel. The received vector has a time-varying instantaneous autocorrelation matrix given by

$$\begin{aligned} \mathbf{R}[n] &\equiv E_C(\mathbf{u}[n]\mathbf{u}^H[n]) \\ &= \tilde{\mathbf{R}} + \mathbf{c}_0[n]\mathbf{c}_0^H[n] \end{aligned} \tag{10}$$

where the correlation matrix of the noise and interference is given by

$$\tilde{\mathbf{R}} = \tilde{\mathbf{C}}\tilde{\mathbf{C}}^H + \sigma_v^2\mathbf{I}. \tag{11}$$

The instantaneous cross-correlation of the received vector and the desired signal is

$$\begin{aligned} \mathbf{p}[n] &\equiv E_C(\mathbf{u}[n]x_0^*[n]) \\ &= \mathbf{c}_0[n]. \end{aligned} \tag{12}$$

B. Time-Varying Channel

It will be important to be able to decompose the channel gain of the fading signal into terms that are dependent and independent of the instantaneous realization of the channel at a given point in time. This decomposition is possible for a Gaussian random process as the decomposition can be done along the lines of correlated and uncorrelated components. This can be applied to the fading channel gain as the Rayleigh random process (the gain magnitude) arises from a two-dimensional (2-D) Gaussian complex gain.

Let $\rho[m]$ be the normalized autocorrelation function of the channel gain; then

$$E(\alpha_0^*[n]\alpha_0[n+m]) = \sigma_0^2\rho[m] \tag{13}$$

In particular, $\rho[m]$ may be the Bessel function of the first kind of zero order that arises from Jakes' model. Note that the normalization by the mean fade power gives $\rho[0] = 1$. The normalized power spectral density (PSD) of the fading process is $P(e^{j\omega})$, which is the Fourier transform of $\rho[n]$.

The stochastic channel gain can be decomposed into terms relative to the realization at time n, giving

$$\alpha_0[n+m] = \rho[m]\alpha_0[n] + \nu_n[n+m]. \tag{14}$$

The complex Gaussian process $\nu_n[k]$ is defined relative to $\alpha_0[n]$, and

$$E(\alpha[n]\nu_n{}^*[k]) = 0 \quad \forall k \tag{15}$$

$$E(\nu_n[k]) = 0 \tag{16}$$

$$E(\nu_n[i]\nu_n{}^*[k]) = \sigma_0^2(\rho[i-k] - \rho[i-n]\rho^*[k-n]). \tag{17}$$

III. Analysis

A. RLS System Definition and Analysis Approximations

The excess MSE due to weight misadjustment is decomposed into contributions from weight lag and weight noise [11]. The lag component arises from the response of the weights to the time-varying channel, whereas the noise component arises due to noisy estimation. The general LS formulation is

$$\hat{\mathbf{R}}[n] = \sum_{k=-\infty}^{\infty} h[n-k]\mathbf{u}[k]\mathbf{u}^H[k] \tag{18}$$

$$\hat{\mathbf{p}}[n] = \sum_{k=-\infty}^{\infty} h[n-k]\mathbf{u}[k]x_0{}^*[k] \tag{19}$$

$$\mathbf{w}[n] = \hat{\mathbf{R}}^{-1}[n]\hat{\mathbf{p}}[n] \tag{20}$$

$$\hat{x}_0[n] = \mathbf{w}^H[n]\mathbf{u}[n]. \tag{21}$$

$$\mathbf{D} = [\mathbf{d}_0 \quad \cdots \quad \mathbf{d}_M] = \begin{bmatrix} 1 & 1 & \cdots & 1 \\ e^{-j2\pi\Delta\cos(\theta_0)} & e^{-j2\pi\Delta\cos(\theta_1)} & & e^{-j2\pi\Delta\cos(\theta_M)} \\ e^{-j4\pi\Delta\cos(\theta_0)} & e^{-j4\pi\Delta\cos(\theta_1)} & & e^{-j4\pi\Delta\cos(\theta_M)} \\ \cdots & & \cdots & \\ e^{-j(2N-2)\pi\Delta\cos(\theta_0)} & e^{-j(2N-2)\pi\Delta\cos(\theta_1)} & & e^{-j(2N-2)\pi\Delta\cos(\theta_M)} \end{bmatrix} \tag{7}$$

The sequence $h[n]$ is herein considered an estimation filter that sums to unity (unit gain at zero frequency) and has a Fourier transform given by $H(e^{j\omega})$. The EW-RLS procedure with an exponential forgetting factor $\lambda < 1$ recursively generates the weighted sample autocorrelation matrix $\hat{\mathbf{R}}$ and cross-correlation vector $\hat{\mathbf{p}}$ with adaptation rate defined as $\beta \equiv 1 - \lambda$, where larger β gives a faster adaptation. As in [19], the performance using the *a priori* weights is considered. Defining the *a priori* estimation filter impulse response $h[n]$ for normalized[1] EW-RLS as

$$h[n] = \begin{cases} 0, & n \leq 0 \\ (1-\lambda)\lambda^{n-1}, & n > 0 \end{cases} \tag{22}$$

the *a priori* estimation error is

$$e[n] = \hat{x}_0[n] - x_0[n]. \tag{23}$$

The instantaneous MSE given the channel and the estimates is[2]

$$\begin{aligned} J_{C,\hat{\mathbf{R}},\hat{\mathbf{p}}}[n] &\equiv E_C\{\,|e[n]|^2 \hat{\mathbf{R}}[n], \hat{\mathbf{p}}[n]\} \\ &= \hat{\mathbf{p}}^H[n]\hat{\mathbf{R}}^{-1}[n]\mathbf{R}[n]\hat{\mathbf{R}}^{-1}[n]\hat{\mathbf{p}}[n] \\ &\quad - \hat{\mathbf{p}}^H[n]\hat{\mathbf{R}}^{-1}[n]\mathbf{p}[n] \\ &\quad - \mathbf{p}^H[n]\hat{\mathbf{R}}^{-1}[n]\hat{\mathbf{p}}[n] + 1 \end{aligned} \tag{24}$$

where $\mathbf{R}[n]$ is the instantaneous statistical autocorrelation matrix, which is still a random function of the random channel. In order to proceed with the tracking analysis, the sample autocorrelation matrix will be assumed to reasonably approximated by considering it to be quasideterministic, given the instantaneous channel

$$\begin{aligned} \hat{\hat{\mathbf{R}}}_D[n] &\equiv E(\hat{\mathbf{R}}[n] \,|\, \mathbf{c}[n-D]) \\ &\cong \hat{\mathbf{R}}[n] \end{aligned} \tag{25}$$

$$\begin{aligned} \hat{\mathbf{R}}^{-1}[n]\mathbf{R}[n]\hat{\mathbf{R}}^{-1}[n] &\cong E(\hat{\mathbf{R}}[n] \,|\, \mathbf{c}[n-D])^{-1} \\ &= \hat{\hat{\mathbf{R}}}_D^{-1}[n] \end{aligned} \tag{26}$$

where D represents some delay relative to the realization time n introduced by the causal estimation. This assumption is an extension from similar assumptions that have been frequently made in previous tracking analyses of RLS systems [16], [11]–[13], where it has been assumed that the sample correlation matrix estimate is exactly the instantaneous statistical autocorrelation matrix. The approximation used herein is more precise in that effects of the estimation filter $h[n]$ and the channel correlation can be considered.

The cross-correlation estimate can be considered to be a perturbation from the true value of the instantaneous cross-correlation.

$$\hat{\mathbf{p}}[n] = \mathbf{c}_0[n] + \mathbf{f}[n] \tag{27}$$

[1]The summations are normalized by $(1-\lambda)$ to conform to the unit zero frequency gain condition, emphasizing the estimation performed and simplifying portraying the error vector/matrix. The two factors cancel in (20); therefore, there is no net effect.

[2]Note that $E(x_0[n]x_0^*[n]) = 1$.

Applying the quasideterministic approximations and taking the expectation over the estimates, the resulting expression is[3]

$$J_C[n] \cong 1 - \mathbf{c}_0^H[n]\hat{\hat{\mathbf{R}}}_D^{-1}[n]\mathbf{c}_0[n] + \mathrm{tr}\left(\hat{\hat{\mathbf{R}}}_D^{-1}[n] E_C(\mathbf{f}[n]\mathbf{f}^H[n])\right) \tag{28}$$

where tr( ) is the trace function, which is the sum of the diagonal components of a matrix.

B. Sample Correlation Matrix Approximation $\hat{\hat{\mathbf{R}}}_D[n]$

The sample autocorrelation matrix approximation (25) captures the effect of the filtering of the "squared" outer vector product. Since each sample vector $\mathbf{u}[n]$ contributes only non-negatively[4] to any eigenvalues of the resultant matrix $\hat{\mathbf{R}}[n]$, this filtered version is less likely to attain nulls than the instantaneous realization of $\mathbf{R}[n]$ itself, which is important when the fading channel gain term $\alpha[n]$ in the inverted matrix may be canceling the channel gain term in $\hat{\mathbf{p}}[n]$. Further, the estimation filter $h[n]$ has a nonzero filter delay, and one would expect that the estimate of $\mathbf{R}[n]$ generated will thus have a certain lag. The approximation defined here allows for some consideration of these effects. It is clear that the expectation of the interferer terms of (25) can extracted from the summation, leaving

$$\hat{\hat{\mathbf{R}}}_D[n] = \tilde{\mathbf{R}} + E\left(\sum_{k=-\infty}^{\infty} h[n-k]\mathbf{c}[k]\mathbf{c}^H[k] \,\middle|\, \mathbf{c}_0[n-D] \right). \tag{29}$$

The channel vector is then decomposed into components that are correlated and uncorrelated with the fading process at time $(n-D)$, according to the decomposition of (14), as is done elsewhere in the lag analysis of Section III-E.

$$\begin{aligned} \hat{\hat{\mathbf{R}}}_D[n] = \tilde{\mathbf{R}} + \mathbf{d}\mathbf{d}^H \cdot E\Bigg(\sum_{k=-\infty}^{\infty} h[n-k]|\rho[k-n+D] \\ \times \alpha[n-D] + \nu_{n-D}[k]|^2 \,\Bigg|\, \alpha[n-D] \Bigg). \end{aligned} \tag{30}$$

Taking this expectation leaves

$$\begin{aligned} \hat{\hat{\mathbf{R}}}_D[n] = \tilde{\mathbf{R}} + \mathbf{d}\mathbf{d}^H \cdot \Bigg(|\alpha[n-D]|^2 \sum_{k=-\infty}^{\infty} h[n-k] \\ \times |\rho[k-n+D]|^2 + \sigma_0^2 \sum_{k=-\infty}^{\infty} h[n-k] \\ \times (1 - |\rho[k-n+D]|^2) \Bigg). \end{aligned} \tag{31}$$

Define the summation $I_{1,2}^{(D)}$

$$I_{1,2}^{(D)} \equiv \sum_{k=-\infty}^{\infty} h[-k]|\rho[k+D]|^2. \tag{32}$$

[3]Here, the matrix relations $\mathrm{tr}(\mathbf{AB}) = \mathrm{tr}(\mathbf{BA})$ and $\mathbf{a}^H\mathbf{B}\mathbf{a} = \mathrm{tr}(\mathbf{a}^H\mathbf{B}\mathbf{a})$ are used, as used repeatedly throughout the analysis.

[4]Note that this statement requires that the filter response $h[n]$ chosen is non-negative as, for example, in standard EW-RLS or rectangular windowed LS. This is required for strictly ensured non-negative definiteness of the resultant estimate.

Equivalently, this can be portrayed in the frequency domain as

$$I_{1,2}^{(D)} = \frac{1}{2\pi}\int_{\omega=-\pi}^{\pi} e^{j\omega D} H(e^{j\omega})(P(e^{j\omega}) \otimes P(e^{j\omega}))\, d\omega \quad (33)$$

where $\otimes$ denotes cyclic convolution. Note that the integral subscripts of $I_{x,y}$ are selected throughout to refer to the order of the filter response x and the PSD y, respectively, in (33) and (56)–(58). The delay argument D appears only when the order of h is unity (i.e., $I_{1,2}^{(D)}$ and $I_{1,1}^{(D)}$) so that there is no temporal symmetry.

Then

$$\hat{\tilde{\mathbf{R}}}_D[n] = \tilde{\mathbf{R}} + \mathbf{d}\mathbf{d}^H \cdot \left(|\alpha[n-D]|^2 I_{1,2}^{(D)} + \sigma_0^2\left(1 - I_{1,2}^{(D)}\right)\right). \quad (34)$$

The inverse of this matrix is considered in Appendix A.

The purpose of incorporating the delay component D is to portray the sample correlation matrix $\hat{\mathbf{R}}[n]$ in a simplified form that captures the relationship between this matrix and the sample cross-correlation vector $\hat{\mathbf{p}}[n]$, and the value of D is selected with this consideration. Setting $D = 0$ is the most simple choice but ignores the delay effects of the estimation filter; another simple but inadequate selection might be the dominant filter group delay, which for EW-RLS is given by $\lambda/(1-\lambda)$ samples at zero frequency. In order to portray $\hat{\mathbf{R}}[n]$ as function of a single instantiation of $\alpha[n-D]$ and best capture the relationship between $\hat{\mathbf{R}}[n]$ and $\hat{\mathbf{p}}[n]$, the delay should be chosen to maximize the residual relationship after taking expectation. This is best accomplished by selecting D to maximize the cross-correlation between the delayed $\alpha[n-D]$ of the correlation matrix and the filtered $\alpha[n]$ of the cross-correlation vector, which is given by $I_{1,1}^{(D)}$ [defined in (57)]. Hence, D is selected to maximize $I_{1,1}^{(D)}$.

It is notable that this approximation to the time-varying sample autocorrelation matrix reduces to the instantaneous statistical autocorrelation when $D = 0$ and $I_{1,2}^{(0)} = 1$ (i.e., the estimation filter is replaced with a delta function in time), providing an approximation similar to that of previous works [11]–[13], [16]; however, as we will discuss later, this approximation would be inadequate to accurately describe the performance of the present system.

C. Characterizing RLS MSE in Terms of Lag and Noise

Let the error involved in each sample cross correlation be $\mathbf{z}[n]$, which consists of the noise and interference terms. It is defined as follows:

$$\mathbf{z}[n] \equiv x_0^*[n] \cdot \left(\sum_{k=1}^{N} x_k[n]\mathbf{c}_k + \mathbf{v}[n]\right). \quad (35)$$

The first and second moments of the cross correlation sample error are then given by

$$E_C(\mathbf{z}[n]) = \mathbf{0} \quad (36)$$

$$E_C(\mathbf{z}[n]\mathbf{z}^H[n-m]) = \tilde{\mathbf{R}}\delta[m]. \quad (37)$$

The lag and noise terms of the sample cross correlation vector error are defined as

$$\mathbf{p}_{\text{lag}}[n] \equiv \sum_{k=-\infty}^{\infty} h[n-k]\mathbf{c}_0[k] - \mathbf{c}_0[n] \quad (38)$$

$$\mathbf{p}_{\text{noise}}[n] \equiv \sum_{k=-\infty}^{\infty} h[n-k]\mathbf{z}[k] \quad (39)$$

and the error vector is given by

$$\mathbf{f}[n] = \mathbf{p}_{\text{lag}}[n] + \mathbf{p}_{\text{noise}}[n]. \quad (40)$$

The lag and noise error vectors are independent so that the autocorrelation of $\mathbf{f}$ is

$$E_C(\mathbf{f}[n]\mathbf{f}^H[n]) = E_C(\mathbf{p}_{\text{lag}}[n]\mathbf{p}_{\text{lag}}{}^H[n]) + E_C(\mathbf{p}_{\text{noise}}[n]\mathbf{p}_{\text{noise}}{}^H[n]). \quad (41)$$

In order to obtain an overall cost measure, the expectation is performed over the channel variation. This final cost, averaged over the channel variations, is

$$J = E(J_C[n]) = J_{\text{opt}} + J_{\text{lag}} + J_{\text{noise}}. \quad (42)$$

From (28), (38), and (39), the components of J are found to be as in (43)–(45), shown at the bottom of the page. It is of interest to compare these results with those of [19]. As in [19], the noise and lag components of the cross-correlation error can be considered to arise from a noise filter $h_{\text{noise}}[n]$ (which is referred to as h_t in [19]) and a lag filter $h_{\text{lag}}[n]$ (which is referred to as h_{te} in [19]), and the summations are convolutions with these filter responses. These two filters produce the combining weight errors from noise and adaptation delay ("lag"). From (38) and (39), these impulse responses are given by

$$h_{\text{noise}}[n] = h[n] \quad (46)$$

$$h_{\text{lag}}[n] = h[n] - \delta[n]. \quad (47)$$

$$J_{\text{opt}} = 1 - E(\mathbf{c}_0{}^H[n]\mathbf{R}^{-1}[n]\mathbf{c}_0[n]) \quad (43)$$

$$J_{\text{lag}} = E(\mathbf{c}_0{}^H[n]\mathbf{R}^{-1}[n]\mathbf{c}_0[n]) + E\left\{\text{tr}\left(\hat{\tilde{\mathbf{R}}}_D^{-1}[n]\sum_{i=-\infty}^{\infty}\sum_{k=-\infty}^{\infty} h[n-k]h\ [n-i]\mathbf{c}_0[i]\mathbf{c}_0{}^H[k]\right)\right\} - E\left\{\text{tr}\left(\hat{\tilde{\mathbf{R}}}_D^{-1}[n]\sum_{i=-\infty}^{\infty} h[n-i]\mathbf{c}_0[i]\mathbf{c}_0^H[n]\right)\right\} - E\left\{\text{tr}\left(\hat{\tilde{\mathbf{R}}}_D^{-1}[n]\sum_{i=-\infty}^{\infty} h[n-i]\mathbf{c}_0[n]\mathbf{c}_0^H[i]\right)\right\} \quad (44)$$

$$J_{\text{noise}} = E\left\{\text{tr}\left(\hat{\tilde{\mathbf{R}}}_D^{-1}[n]\sum_{i=-\infty}^{\infty}\sum_{k=-\infty}^{\infty} h[n-i]\ \ h[n-k]\delta[i-k]\tilde{\mathbf{R}}\right)\right\}. \quad (45)$$

Thus, with $\otimes$ here denoting time convolution

$$\mathbf{f}[n] = h_{\text{lag}}[n] \otimes \mathbf{c}_0[n] + h_{\text{noise}}[n] \otimes \mathbf{z}[n]. \tag{48}$$

In contrast to the system identification analysis of [19], this result is not yet definitive since in the analysis of [19], the autocorrelation matrix $\mathbf{R}[n]$ is explicitly assumed to be time invariant based on the statistics of the source. In the context of system identification, this is a reasonable assumption. However, this condition is clearly not valid for the interference cancellation application now under analysis. The MSE cannot be characterized using only these filter values because there is an interaction between the time variation of the correlation matrix and the cross-correlation vector. This is made explicit when considering that $\hat{\mathbf{R}}_D[n]$ and $\mathbf{R}[n]$ in (43)–(45) are both functions of the sequence $\mathbf{c}_0[n]$, which also appears in the sample cross-correlation error summations. Thus, the present problem requires a more rigorous consideration of the interplay between these functions. This is presented in the following sections.

D. Optimal Time Varying Wiener Combiner

The MSE performance of the time varying Wiener combiner with no tracking error was given in (43). Using the matrix inversion lemma result (77) from Appendix A gives

$$J_{\text{opt}} = 1 - E\left(\frac{|\alpha_0[n]|^2}{\gamma + |\alpha_0[n]|^2}\right) \tag{49}$$

where $\alpha_0[n]$ is complex Gaussian so that $|\alpha_0[n]|^2$ follows an exponential distribution with mean σ_0^2, and

$$E\left(\frac{|\alpha_0[n]|^2}{\gamma + |\alpha_0[n]|^2}\right) = \frac{\gamma}{\sigma_0^2} e^{\gamma/\sigma_0^2} \text{Ei}\left(-\gamma/\sigma_0^2\right) + 1 \tag{50}$$

and

$$J_{\text{opt}} = -\frac{\gamma}{\sigma_0^2} e^{\gamma/\sigma_0^2} \text{Ei}\left(-\gamma/\sigma_0^2\right) \tag{51}$$

where Ei( ) is the exponential integral function [23].

E. Excess MSE Due to Lag

The lag term (44) of the MSE is the most complicated as it incorporates the interaction of the channel variation in the cross-correlation vector and in the autocorrelation matrix.

Recall that the angular dispersion of the arriving multipath is assumed to be very small (see Fig. 2), giving rise to correlated fading across all of the antenna elements. In this case, there is no diversity gain (only beam forming gain). This simplification allows us to decompose the correlation matrix and apply the matrix inversion lemma as in Appendix A. Then, using the results of (77) with (34) but separating $\alpha_0[\cdot]$, where it cannot be extracted from the summation, (44) becomes

$$J_{\text{lag}} = E\left(\frac{|\alpha_0[n]|^2}{\gamma + |\alpha_0[n]|^2}\right) + E\left(\frac{\sum_{i=-\infty}^{\infty}\sum_{k=-\infty}^{\infty} h[n-i]h[n-k]\alpha_0[i]\alpha_0^*[k]}{\gamma + \sigma_0^2\left(1 - I_{1,2}^{(D)}\right) + |\alpha[n-D]|^2 I_{1,2}^{(D)}}\right) - 2E\left(\frac{\sum_{i=-\infty}^{\infty} h[n-i]\text{Re}(\alpha_0[i]\alpha_0^*[n])}{\gamma + \sigma_0^2\left(1 - I_{1,2}^{(D)}\right) + |\alpha[n-D]|^2 I_{1,2}^{(D)}}\right). \tag{52}$$

Then, $\alpha_0[i]$ is decomposed relative to time $(n - D)$, as in (14), such that the expectation can be separated along the lines of independent components, as in (53), shown at the bottom of the page. Extracting $\alpha_0[n - D]$ from the summation, taking the expectation within the summation using the autocorrelation of the orthogonal process $\nu_n[\cdot]$ (17), and discarding the vanishing cross terms gives (54), shown at the bottom of the next page. The form of (54) shows that the effects of the channel gain PDF have been decoupled from the effects of the channel gain autocorrelation. Further analysis is then broken into finding the expectation, which characterizes the channel PDF, and computing the summations, which contain the channel correlation function. A similar decoupling could be found for Ricean or Nakagami fading PDF as they can both be characterized by Gaussian processes.

Of the expectations in (54), one was already considered (50), and the other is given by

$$E\left(\frac{1}{\gamma + \sigma_0^2\left(1 - I_{1,2}^{(D)}\right) + |\alpha[n-D]|^2 I_{1,2}^{(D)}}\right) = -\frac{1}{I_{1,2}^{(D)}\sigma_0^2} \exp\left(\frac{\gamma + \sigma_0^2\left(1 - I_{1,2}^{(D)}\right)}{I_{1,2}^{(D)}\sigma_0^2}\right) \times \text{Ei}\left(-\frac{\gamma + \sigma_0^2\left(1 - I_{1,2}^{(D)}\right)}{I_{1,2}^{(D)}\sigma_0^2}\right). \tag{55}$$

Define inverse transform integrals for $n = 0$

$$I_{2,1} \equiv \frac{1}{2\pi}\int_{-\pi}^{\pi} |H(e^{j\omega})|^2 P(e^{j\omega})\, d\omega \tag{56}$$

$$I_{1,1}^{(D)} \equiv \frac{1}{2\pi}\int_{-\pi}^{\pi} e^{jD\omega} H(e^{j\omega}) P(e^{j\omega})\, d\omega \tag{57}$$

$$J_{\text{lag}} = E\left(\frac{|\alpha_0[n]|^2}{\gamma + |\alpha[n]|^2} + \frac{\sum_{i=-\infty}^{\infty}\sum_{k=-\infty}^{\infty} h[n-k]h[n-i](\rho[i-n+D]\alpha_0[n-D] + \nu_{n-D}[i])(\rho^*[k-n+D]\alpha_0^*[n-D] + \nu_{n-D}^*[k])}{\gamma + \sigma_0^2\left(1 - I_{1,2}^{(D)}\right) + |\alpha[n-D]|^2 I_{1,2}^{(D)}} - \frac{2\sum_{i=-\infty}^{\infty} h[n-i]\text{Re}((\rho[i-n+D]\alpha_0[n-D] + \nu_{n-D}[i])(\rho^*[D]\alpha_0^*[n-D] + \nu_{n-D^*}[n]))}{\gamma + \sigma_0^2\left(1 - I_{1,2}^{(D)}\right) + |\alpha[n-D]|^2 I_{1,2}^{(D)}}\right). \tag{53}$$

$$I_{2,0} \equiv \frac{1}{2\pi}\int_{-\pi}^{\pi} |H(e^{j\omega})|^2\, d\omega. \tag{58}$$

Applying the results for the expeetations (50), (55), and the frequeney domain integrals (56)–(58) yields

$$\begin{aligned} J_{\text{lag}} = {} & \frac{\gamma}{\sigma_0^2} e^{\gamma/\sigma_0^2}\,\text{Ei}\left(-\gamma/\sigma_0^2\right) + 1 \\ & + \frac{1}{I_{1,2}^{(D)}}\left(\left|I_{1,1}^{(D)}\right|^2 - 2\text{Re}\left(\rho^*[D] I_{1,1}^{(D)}\right)\right) \\ & \times \left(\frac{\gamma + \sigma_0^2\left(1 - I_{1,2}^{(D)}\right)}{I_{1,2}^{(D)}\sigma_0^2}\exp\left(\frac{\gamma + \sigma_0^2\left(1 - I_{1,2}^{(D)}\right)}{I_{1,2}^{(D)}\sigma_0^2}\right)\right. \\ & \left. \times\, \text{Ei}\left(-\frac{\gamma + \sigma_0^2\left(1 - I_{1,2}^{(D)}\right)}{I_{1,2}^{(D)}\sigma_0^2}\right) + 1\right) \\ & + \frac{1}{I_{1,2}^{(D)}}\left(\left|I_{1,1}^{(D)}\right|^2 + 2\text{Re}\left(I_{1,1}^{(0)} - \rho^*[D] I_{1,1}^{(D)}\right) - I_{2,1}\right) \\ & \times \exp\left(\frac{\gamma + \sigma_0^2\left(1 - I_{1,2}^{(D)}\right)}{I_{1,2}^{(D)}\sigma_0^2}\right) \\ & \times \text{Ei}\left(-\frac{\gamma + \sigma_0^2\left(1 - I_{1,2}^{(D)}\right)}{I_{1,2}^{(D)}\sigma_0^2}\right). \end{aligned} \tag{59}$$

Equation (59) provides the MSE contribution due to lag, incorporating the ehannel fading eorrelation funetion in the integrals (56)–(58) so that the lag MSE ean be quiekly obtained for different mobility rates or ehannel assumptions.

F. Excess MSE Due to Weight Noise Error

The exeess MSE due to weight noise error was given in (45). Again, deeomposing $\hat{\tilde{\mathbf{R}}}[n-D]$ and applying the matrix inversion lemma gives

$$\begin{aligned} J_{\text{noise}} = {} & \sum_{i=-\infty}^{\infty}\sum_{k=-\infty}^{\infty} h[n-i]h[n-k]\delta[i-k] \\ & - E\left(\frac{|\alpha_0[n-D]|^2}{\gamma + \sigma_0^2\left(1 - I_{1,2}^{(D)}\right) + |\alpha[n-D]|^2 I_{1,2}^{(D)}}\right) \\ & \times \sum_{i=-\infty}^{\infty}\sum_{k=-\infty}^{\infty} h[n-i]h[n-k]\delta[i-k]. \end{aligned} \tag{60}$$

Through similar procedures to those used for the lag ealeulation and using (50)

$$\begin{aligned} J_{\text{noise}} = {} & -\frac{I_{2,0}}{I_{1,2}^{(D)}} \cdot \frac{\gamma + \sigma_0^2\left(1 - I_{1,2}^{(D)}\right)}{I_{1,2}^{(D)}\sigma_0^2} \\ & \times \exp\left(\frac{\gamma + \sigma_0^2\left(1 - I_{1,2}^{(D)}\right)}{I_{1,2}^{(D)}\sigma_0^2}\right) \\ & \times \text{Ei}\left(-\frac{\gamma + \sigma_0^2\left(1 - I_{1,2}^{(D)}\right)}{I_{1,2}^{(D)}\sigma_0^2}\right). \end{aligned} \tag{61}$$

From (61), it is seen that the PSD of the fading ehannel does not affeet the noise misadjustment term, although the PDF of the ehannel gain is ineorporated.

$$\begin{aligned} J_{\text{lag}} = {} & E\left(\frac{|\alpha_0[n]|^2}{\gamma + |\alpha[n]|^2}\right) \\ & + E\left(\frac{|\alpha_0[n-D]|^2}{\gamma + \sigma_0^2\left(1 - I_{1,2}^{(D)}\right) + |\alpha[n-D]|^2 I_{1,2}^{(D)}}\right) \sum_{i=-\infty}^{\infty}\sum_{k=-\infty}^{\infty} h[n-i]h[n-k] \\ & \times \rho[i-n+D]\rho^*[k-n+D] \\ & + \sigma_0^2 E\left(\frac{1}{\gamma + \sigma_0^2\left(1 - I_{1,2}^{(D)}\right) + |\alpha[n-D]|^2 I_{1,2}^{(D)}}\right) \sum_{i=-\infty}^{\infty}\sum_{k=-\infty}^{\infty} h[n-i]h[n-k]\rho[i-k] \\ & - \sigma_0^2 E\left(\frac{1}{\gamma + \sigma_0^2\left(1 - I_{1,2}^{(D)}\right) + |\alpha[n-D]|^2 I_{1,2}^{(D)}}\right) \sum_{i=-\infty}^{\infty}\sum_{k=-\infty}^{\infty} h[n-i]h[n-k] \\ & \times \rho[i-n+D]\rho^*[k-n+D] \\ & - 2E\left(\frac{|\alpha_0[n-D]|^2}{\gamma + \sigma_0^2\left(1 - I_{1,2}^{(D)}\right) + |\alpha[n-D]|^2 I_{1,2}^{(D)}}\right) \text{Re}\left(\rho^*[D] \cdot \sum_{i=-\infty}^{\infty} h[n-i]\rho[i-n+D]\right) \\ & - 2\sigma_0^2 E\left(\frac{1}{\gamma + \sigma_0^2\left(1 - I_{1,2}^{(D)}\right) + |\alpha[n-D]|^2 I_{1,2}^{(D)}}\right) \sum_{i=-\infty}^{\infty} h[n-i]\text{Re}(\rho[n-i]) \\ & + 2\sigma_0^2 E\left(\frac{1}{\gamma + \sigma_0^2\left(1 - I_{1,2}^{(D)}\right) + |\alpha[n-D]|^2 I_{1,2}^{(D)}}\right) \sum_{i=-\infty}^{\infty} h[n-i]\text{Re}(\rho^*[D]\rho[i-n+D]). \end{aligned} \tag{54}$$

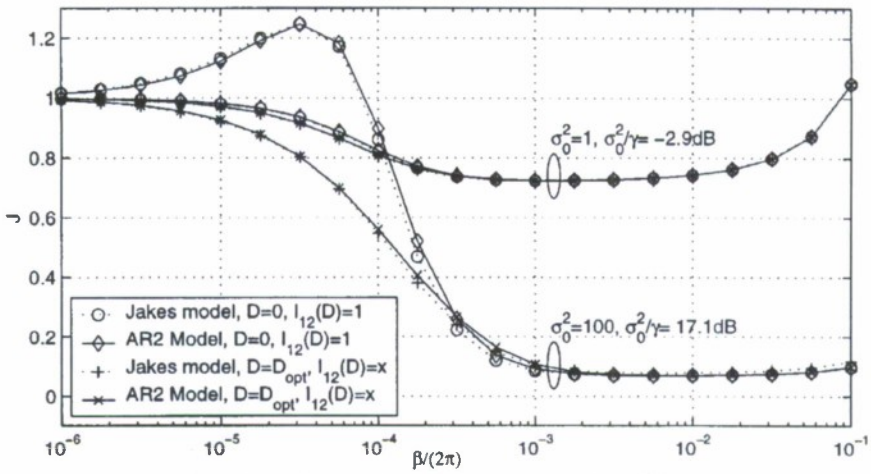

Fig. 3. Comparison of results for Jakes model (69) and the AR2 model (71)–(74) with ($D = 0$, fixed $I_{1,2}^{(0)} = 1$), and with ($D = D_{\text{opt}}, I_{1,2}^{(D)} = x$, denoting normal calculation). $I_{1,2}^{(D)}$ calculated numerically for Jakes' spectrum. Doppler frequency of $f_d = 1e-4$ cycles/sample. Shown for varying SNR.

G. Summary of MSE in Rayleigh Fading

The MSE of the RLS antenna array system has been decomposed into the Wiener MSE, excess MSE due to lag misadjustment, and excess MSE due to noise misadjustment. The overall MSE of the system is given by the summation of these three MSE terms, which is given by (51), (59), and (61). The analysis has allowed for the separation of the complex Gaussian fading gain PDF from the PSD of the fading process. The effects of the time correlation of the fading process are captured in the four integrals (33), (56), (57), and (58). The "optimal" value of D is termed D_{opt} and selected to maximize $I_{1,1}^{(D)}$, as discussed in Section III–B. The MSE is calculated as

$$D = D_{\text{opt}} \equiv \arg\left(\max_x \left|I_{1,1}^{(x)}\right|\right) \tag{62}$$

$$\begin{aligned} J = 1 &+ \frac{\left(\left|I_{1,1}^{(D)}\right|^2 - 2\text{Re}\left(\rho^*[D]I_{1,1}^{(D)}\right) - I_{2,0}\right)}{I_{1,2}^{(D)}} \\ &\times \left(\frac{\gamma + \sigma_0^2\left(1 - I_{1,2}^{(D)}\right)}{I_{1,2}^{(D)}\sigma_0^2}\exp\left(\frac{\gamma + \sigma_0^2\left(1 - I_{1,2}^{(D)}\right)}{I_{1,2}^{(D)}\sigma_0^2}\right)\right. \\ &\left.\times \text{Ei}\left(-\frac{\gamma + \sigma_0^2\left(1 - I_{1,2}^{(D)}\right)}{I_{1,2}^{(D)}\sigma_0^2}\right) + 1\right) \\ &+ \frac{\left(\left|I_{1,1}^{(D)}\right|^2 + 2\text{Re}\left(I_{1,1}^{(0)} - \rho^*[D]I_{1,1}^{(D)}\right) - I_{2,1}\right)}{I_{1,2}^{(D)}} \\ &\times \exp\left(\frac{\gamma + \sigma_0^2\left(1 - I_{1,2}^{(D)}\right)}{I_{1,2}^{(D)}\sigma_0^2}\right) \\ &\times \text{Ei}\left(-\frac{\gamma + \sigma_0^2\left(1 - I_{1,2}^{(D)}\right)}{I_{1,2}^{(D)}\sigma_0^2}\right). \end{aligned} \tag{63}$$

IV. Numerical Examples

A. Jakes' Model Fading

For the Jakes' model [22], approximate closed-form results are available using the simplified case where $D = 0$ and with artificially fixed $I_{1,2}^{(0)} = 1$. The Jakes' PSD is

$$P_{\text{jakes}}(e^{j\omega}) = \begin{cases} \frac{2}{\sqrt{\omega_d^2 - \omega^2}}, & |\omega| < \omega_d \\ 0, & |\omega| \geq \omega_d \end{cases} \tag{64}$$

$$\rho_{\text{jakes}}[n] = J_0(\omega_d n) \tag{65}$$

where ω_d is the Doppler frequency, and $J_0(x)$ is the zero-order Bessel function of the first kind.

For the filter of (22) and PSD of (64), the integrals (56) and (57) can be found with $D = 0$ for small ω_d by using the approximation $z \cong 1 + j\omega$, and where appropriate, $\lambda \cong 1$.

$$\begin{aligned} I_{2,1} &\cong \frac{1}{2\pi}\int_{-\omega_d}^{\omega_d} \frac{\beta^2}{\beta^2 + \omega^2}\frac{2}{\sqrt{\omega_d^2 - \omega^2}}\,d\omega \\ &= \frac{\beta}{\sqrt{\beta^2 + \omega_d^2}} \end{aligned} \tag{66}$$

$$\begin{aligned} I_{1,1}^{(0)} &\cong \frac{1}{2\pi}\int_{-\omega_d}^{\omega_d} \frac{\beta^2 - j\beta\omega}{\beta^2 + \omega^2}\frac{2}{\sqrt{\omega_d^2 - \omega^2}}\,d\omega \\ &= I_{2,1}. \end{aligned} \tag{67}$$

The final integral (58) is given by

$$\begin{aligned} I_{2,0} &= \frac{(1-\lambda)}{(1+\lambda)} \\ &= \frac{\beta}{2-\beta}. \end{aligned} \tag{68}$$

Hence, with fixed $I_{1,2}^{(0)} = 1$, the MSE of the system is given by

$$\begin{aligned} J|_{D=0} = &-\frac{\gamma}{\sigma_0^2}e^{\gamma/\sigma_0^2}\text{Ei}\left(-\gamma/\sigma_0^2\right) \\ &+ \left(\frac{\beta}{\sqrt{\beta^2 + \omega_d^2}} - 1\right)^2 \cdot \left(\frac{\gamma}{\sigma_0^2}e^{\gamma/\sigma_0^2}\text{Ei}\left(-\gamma/\sigma_0^2\right) + 1\right) \\ &+ \left(\frac{\beta}{\sqrt{\beta^2 + \omega_d^2}} - \frac{\beta^2}{\beta^2 + \omega_d^2}\right) \cdot \left(-e^{\gamma/\sigma_0^2}\text{Ei}\left(-\gamma/\sigma_0^2\right)\right) \\ &- \frac{\beta}{2-\beta} \cdot \left(\frac{\gamma}{\sigma_0^2}e^{\gamma/\sigma_0^2}\text{Ei}\left(-\gamma/\sigma_0^2\right)\right). \end{aligned} \tag{69}$$

This MSE result is compared with that of the AR2 model (see Section IV-B) in Fig. 3. Evaluation of the integrals for the general case $D \neq 0$ and/or realistic $I_{1,2}^{(D)}$ must be done numerically.

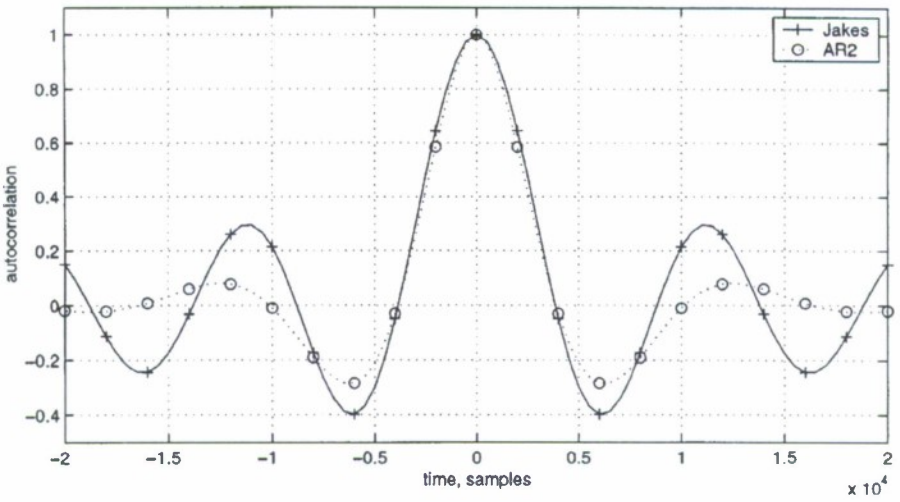

Fig. 4. Autocorrelation of Jakes' model and AR2 approximation $f_d = 0.0001$ cycles/sample.

B. AR2 Fading

In order to provide tractable mathematical expressions for this numerical example, the Jakes' model will be approximated as a second-order autoregressive process (AR2), with poles selected to provide a PSD close to that of the Jakes' model. This model provides not only an analytic solution but a simple implementation for simulation. A good match between the Jakes' correlation and the AR2 correlation for small time offsets is found by selecting the poles according to the rule

$$p = \left(1 - \frac{\omega_d}{\pi}\right) \exp(\pm j \cdot 0.8 \cdot \omega_d) \tag{70}$$

where ω_d is the discrete time Doppler frequency, and the poles are in the z-plane. The AR2 process and the resulting PSD is described in more detail in Appendix C.

By way of a specific example, consider a system with a 1 MHz signal bandwidth and 100 Hz fading, as would arise from a velocity of 67 mi/h (108 km/h) with a carrier frequency of 1 GHz. In the discrete time domain after sampling at the 1 MHz Nyquist rate, these parameters give a fading rate of $1e-4$ cycles/sample or $\omega_d = 2\pi \cdot 1e-4$ rad/sample. The AR model is then defined with poles at $0.9998 \cdot \exp(\pm j 2\pi \cdot 0.000\,08)$. The resultant autocorrelation is shown in Fig. 4. Simulations are also run with $f_d = 5e-4$ cycles/sample for comparison.

For an AR2 process with poles at p and p^*, the integral values are given in (71)–(74), shown at the bottom of the page, using the AR2 nomenclature of Appendix C.

Plugging (71)–(74) into (63) provides a closed-form value of the MSE at the output of the antenna array combiner.

C. Simulation and Discussion

Simulations were performed with the AR2 model in order to confirm the analysis. The simulation results are compared to several analytic configurations, which show that the delay term D must be properly selected as described in (62), and $I_{1,2}^{(D)}$ cannot be simplified to unity but rather must be explicitly determined. Since ultimately a metric such as bit error rate is of in-

$$I_{1,2}^{(D)} = \frac{(1-\lambda)\lambda^D}{1+\cos(2\psi)} \cdot \left(\frac{\lambda^{-1}r^2 - \lambda^{-D-1}r^{2D+2}}{1-\lambda^{-1}r^2} + \frac{1}{1-\lambda r^2} + \frac{\lambda^{-1}r^2\cos(2\psi+2\theta) - \lambda^{-D-1}r^{2D+2}\cos(2\psi+2D\theta+2\theta) - \lambda^{-2}r^4\cos(2\psi) + \lambda^{-D-2}r^{2D+4}\cos(2D\theta+2\psi)}{1-2\lambda^{-1}r^2\cos(2\theta)+\lambda^{-2}r^4} + \frac{\cos(2\psi) - \lambda r^2\cos(-2\theta+2\psi)}{1-2\lambda r^2\cos(2\theta)+\lambda^2 r^4} \right) \tag{71}$$

$$I_{2,1} = \frac{(1-\lambda)\cdot(1-r^2)\cdot|1-p^2|\sin(\theta)}{(1+\lambda)(1-p\lambda)(\lambda-p)(1-p^*\lambda)(\lambda-p^*)\sin(\theta-\text{angle}(1-p^2))} \cdot \lambda^2 + \frac{(1-\lambda)^2\sin(2\theta-\text{angle}((1-p^2)(1-\lambda p)(\lambda-p)))}{|1-\lambda p||\lambda-p|\sin(\theta-\text{angle}(1-p^2))} \cdot r^2 \tag{72}$$

$$I_{1,1}^{(D)} = \begin{cases} \frac{(1-\lambda)}{|1-\lambda p|\cos(\psi)} r^{-D+2}\sin(-D\theta+2\theta+\text{angle}((1-\lambda p)(1-p^2))) & D \le 2 \\ \frac{(1-\lambda)\sin(\theta)(1-r^2)|1-p^2|}{\cos(\psi)(\lambda^2-2\lambda r\cos(\theta)+r^2)(1-2\lambda r\cos(\theta)+\lambda^2 r^2)}\lambda^{D+1} & \\ \quad -\frac{(1-\lambda)}{\cos(\psi)|\lambda-p|} r^{D+1}\sin(D\theta+\theta-\text{angle}((\lambda-p)(1-p^2))) & D > 2 \end{cases} \tag{73}$$

$$I_{2,0} = \frac{1-\lambda}{1+\lambda} \tag{74}$$

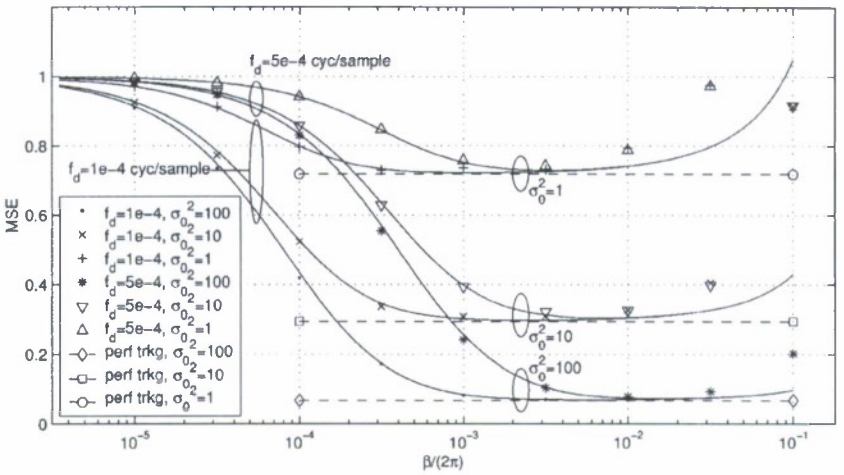

Fig. 5. MSE from analysis (solid lines) and simulation (points). Doppler frequencies $1e-4, 5e-4$ cycles/sample, as indicated.

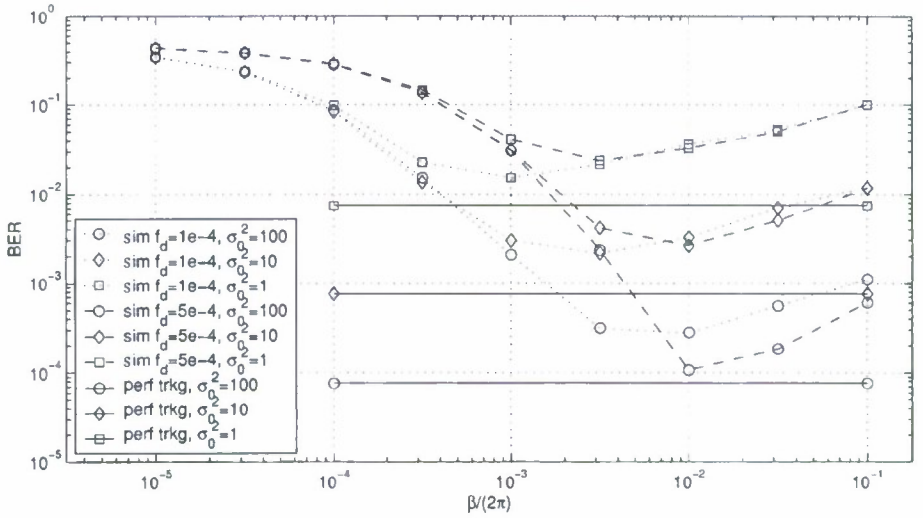

Fig. 6. Cross-over probability (BER) from simulation. Doppler frequencies $1e-4, 5e-4$. Perfect tracking lines are according to Gaussian interference approximation with fading constant throughout a bit symbol.

terest, BER was extracted from the simulation in addition to the MSE. The simulation implemented a pseudo-CDMA system, as shown in Fig. 1, where the signal is known by both receiver and transmitter in order to facilitate tracking, as is the case when a training sequence or pilot is available. Since the signal is known in this case, there are no information bits to extract. To extract a BER metric, bit decisions are modeled as a crossover decision. For CDMA reception, the signal is multiplied by a code ($x^*[n]$) and accumulated. In this case, the "data" is all $+1$s; therefore, if the accumulator output is greater than zero, then there is no detection error, and if it is less than zero, then there is a detection error. This can equivalently be considered to be a system with perfect decision-directed feedback. This provides an adequate model for a general evaluation of the tracking performance of the system.

It is assumed that each transmitter is power controlled so that the average power received by the base station from each mobile is the same, but the desired signal mean power σ_0^2 is varied over [1 10 100] to better illustrate the BER performance. The interferers experience a static channel with unit mean received power, and the desired signal undergoes Rayleigh fading. The antenna array is comprised of three elements, spaced 0.4 wavelengths apart. The desired transmitter has an angle-of-arrival (AOA) of 108°, and there are eight interferers with randomly assigned AOAs of 32°, 73°, 111°, 133°, 143°, 157°, 165°, 166°, and 168°. No AWGN is applied to the received vector; therefore, all noise considered is due to the interferers; this emphasizes the gains from null forming.

With these parameters, the effective signal to noise is $0.125 \cdot \sigma_0^2$ with one antenna, whereas with the three antennas, one can obtain

$$E(|\alpha_0[n]|^2) \cdot \mathbf{d}_0^H \tilde{\mathbf{R}}^{-1} \mathbf{d}_0 = 0.512\sigma_0^2.$$

This is a 6.1 dB improvement over the single antenna case.

The simulations were run using AR2 fading rates of $1e-4$ and $5e-4$ cycles/sample. The results are seen in Figs. 5 and 6, which show the mean square error and bit error rate of the system as a function of the adaptation rate β. Noting that β is the 3 dB bandwidth in units of rad/sample of the estimation filter, the x-axes

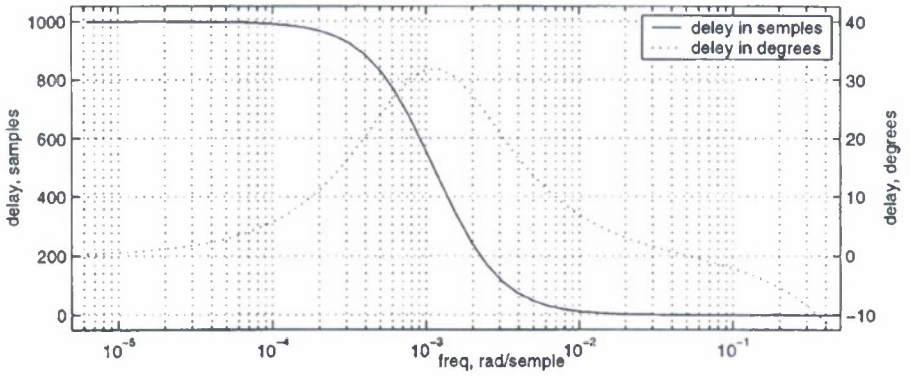

Fig. 7. Group delay of estimation filter $H(e^{j\omega})$ with $\beta = 1e-3$ (3 dB bandwidth $(2\pi)^{-1} \cdot 1e-3$ cycles/sample).

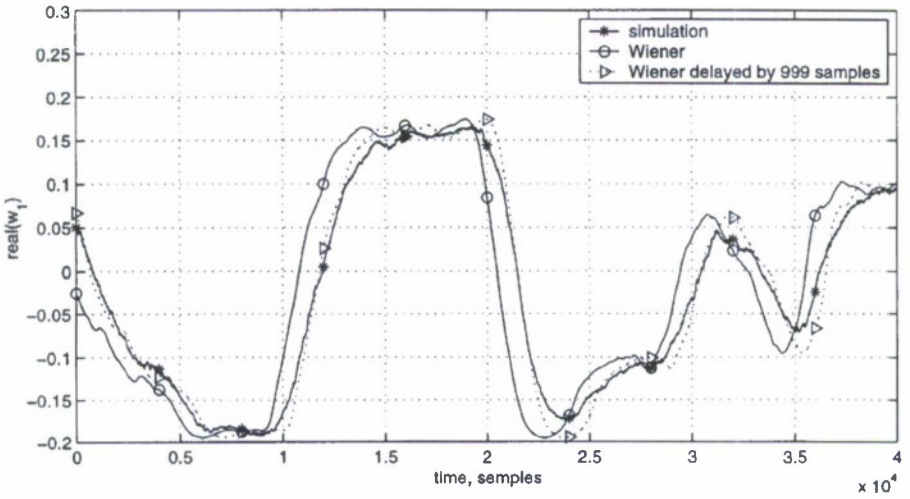

Fig. 8. Time-varying combiner weight, illustrating the weight delay. $\sigma_0^2 = 1, \sigma_0^2/\gamma = -2.9$ dB, $f_d = 1e-4, \beta = 1e-3$, delay = 999 samples. Real component of w_1 is shown.

are scaled by $1/2\pi$. The MSE simulations match the analysis for smaller β, becoming less accurate for larger β, where the noisy sample autocorrelation matrix degrades performance and the quasideterministic assumption breaks down.

Both the analysis and simulations indicate that in order to attain reasonable performance, the 3 db bandwidth arising from β must be selected to be about an order of magnitude larger than the Doppler frequency (Figs. 5 and 6). To consider why so much margin is needed in β, consider the filter response $H(e^{j\omega})$. The delay of the estimation filter $h[n]$ at low frequencies is $(1-\beta)/\beta$ samples, shown in Fig. 7. This delay is seen to be very significant near the transition band when considered in units of degrees. Thus, the large margin in the value of β is required to accommodate this delay, which, otherwise, will cause lag error in the combiner. A plot of one of the time-varying weights, along with the optimal weight and a delayed version of the optimal weight, is given in Fig. 8. As the problem formulation is similar across the weights, showing one weight is adequate for qualitative visualization. This figure clearly shows that for moderate lag errors, the lag takes the form of a minimally distorted but delayed version of the optimal weights, and the zero frequency filter delay of $(1-\beta)/\beta$, which is 999 samples in the figure, characterizes this delay well. Most of the fading process power is near the edge of the band, where the group delay effects are strongest, exacerbating this problem. The plot of delay in degrees (see Fig. 7) shows that about one decade of margin between Doppler frequency to the filter 3 dB bandwidth is required in order to avoid this lag effect. It is also of interest to note that the BER performance of the $5e-4$ cycles/sample Doppler case is actually lower for higher SNR than the $1e-4$ cycles/sample case when $\beta = 2\pi \cdot 1e-2$, counter to expectations in a tracking problem; this is due to time diversity as the very deep fades that produce bit errors at high SNRs are also very brief, and at faster fading rates, the fades do not annihilate the entire 64-chip symbol.

Fig. 9 shows MSE simulated and calculated with various values of D and $I_{1,2}^{(D)}$, demonstrating that the formulation of the complete analysis is required for accurate results. With the "optimal" D and calculated $I_{1,2}^{(D)}$, the results closely match the simulation. The simplest form to calculate would be $D = 0$ and artificially set $I_{1,2}^{(D)} = 1$; this form gives large peaking when the Doppler frequency falls in the estimation filter transition band. Letting $D = D_{\text{opt}}$ and setting $I_{1,2}^{(D)} = 1$ also results in a large error. The error in these cases is particularly large for high SNRs because here, the correct handling of the cancellation of the $\alpha[n]$ terms in the inverted autocorrelation matrix $\mathbf{R}$ and

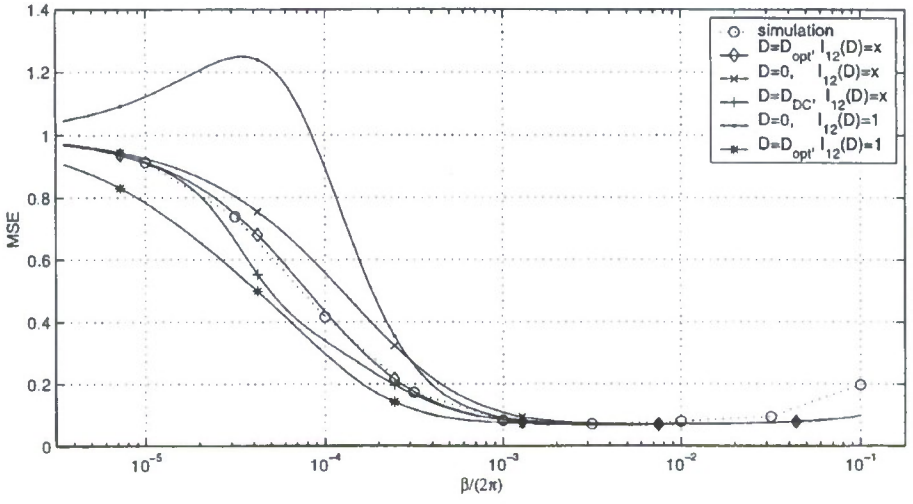

Fig. 9. MSE calculations for various values D and $I_{1,2}^{(D)}$, $\sigma^2 = 100$. $D_{\rm opt}$ is the value of D that maximizes $I_{1,1}^{(D)}$. $D_{\rm DC} = \lambda/(1-\lambda)$ is the filter group delay at zero frequency; $I_{1,1}^{(D)} = x$ indicates normal calculation; $I_{1,1}^{(D)} = 1$ fixes the value to unity.

the cross-correlation vector $\mathbf{p}$ becomes more important. The filtering present in the sample autocorrelation matrix $\hat{\mathbf{R}}$ means that even when the signal fades, there is residual filtered signal in the sample autocorrelation matrix so that near divide-by-zero conditions are avoided in the realized $\hat{\mathbf{R}}$; this motivates the definition of $\hat{\hat{\mathbf{R}}}$, which leaves a "lagged residual" of $\alpha[n]$ in the form of the $((1 - I_{1,2}^{(D)})\sigma_0^2)$ term. It is also clear from the figure that the selection of the value of D is important.

The result for the AR2 model [see (71)–(74)] is compared with the result for the Jakes' model [see (69)] in Fig. 3 with the simplifying conditions $D = 0$ and fixed $I_{1,2}^{(D)} = 1$. As discussed above, these conditions do not allow a very accurate prediction of the performance, but the closed-form approximate result for the Jakes' model is available. Results obtained by numerical integration for the Jakes' model are also displayed for the most accurate formulation [see (62) and (63)]. The calculated MSE for the Jakes' and AR2 models are nearly identical, illustrating that the use of an AR2 approximation to Jakes' is appropriate.

The performance is limited by the exponential weighting of the EW-RLS estimates. We have surmised that this is largely due to the phase shift imposed by the exponential filter. Lin *et al.* [19] suggested optimal weighting functions to replace the exponential weighting for the identification problem. Results similar to those could be found here from (63). However, the significance of this would be obscured by the complexity of the equations involved.

It is of interest to compare the present tracking results with those derived for system identification of a Jakes fading channel [19] and the first-order Markov process [16], as well as for prediction of a chirped process [12]. The noise misadjustment is found to be approximately proportional to β in all of these cases, which is in agreement with (74). The lag misadjustment in [16] is found to be inversely proportional to β, whereas in [19] and [12], it is found to be inversely proportional to β^2. From (71)–(74), it is clear that no such simplification is, in general, possible for the interference canceling mobile wireless communications problem. The lag misadjustment is a function of the fading PSD and, in general, cannot be reduced to some simple polynomial of β.

V. Conclusion

This paper has presented a derivation of the MSE that results from the application of the EW-RLS algorithm to an antenna array receiving signals degraded by a Rayleigh fading channel. It is shown that the time correlation of the fading channel can be extracted from the probability density function of the channel such that the exponential weighting used for the cross-correlation estimate could be considered to be a filtering operation. Considering the windowing function to be a filtering operation allows the application of well-known Fourier analysis techniques so that the analysis can be conveniently applied to channels with different fading PSDs.

The application of Fourier analysis is similar to [19] but is applicable to the "interference canceling" tracking problem that characterizes the antenna array problem. This paper expands the use of such techniques, illustrating a methodology for applying such analysis when the correlation matrix of the received vector is time varying, as is frequently the case in communications problems.

Appendix A
Autocorrelation Matrix Inverse Decompositions

A. Decomposition of the Inverse of the Statistical Correlation Matrix $\boldsymbol{R}[n]$

It is frequently necessary throughout the analysis to separate the contributions of the desired signal and the interferers to the autocorrelation matrix inverse. This can be accomplished through straightforward application of the matrix inversion lemma.

The decomposed correlation matrix is given by (10). The matrix inversion lemma applied to (10) gives

$$\mathbf{R}^{-1}[n] = \tilde{\mathbf{R}}^{-1} - \frac{\tilde{\mathbf{R}}^{-1}\mathbf{c}_0[n]\mathbf{c}_0^H[n]\tilde{\mathbf{R}}^{-1}}{1 + \mathbf{c}_0^H[n]\tilde{\mathbf{R}}^{-1}\mathbf{c}_0[n]}. \tag{75}$$

The inner product of the channel response with respect to the inverse of the correlation matrix can be reduced to a simple form.

$$\mathbf{c}_0^H[n]\mathbf{R}^{-1}[n]\mathbf{c}_0[n] = \frac{\mathbf{c}_0^H[n]\tilde{\mathbf{R}}^{-1}\mathbf{c}_0[n]}{1+\mathbf{c}_0^H[n]\tilde{\mathbf{R}}^{-1}\mathbf{c}_0[n]}. \quad (76)$$

Given the narrow angular dispersion of the channel model, this reduces to

$$\mathbf{c}_0^H[n]\mathbf{R}^{-1}[n]\mathbf{c}_0[n] = \frac{|\alpha_0[n]|^2}{\gamma+|\alpha_0[n]|^2} \quad (77)$$

where γ provides a sense of the irreducible noise power projected into the signal space.

$$\frac{1}{\gamma} \equiv \mathbf{d}_0^H\tilde{\mathbf{R}}^{-1}\mathbf{d}_0. \quad (78)$$

B. Decomposition of the Inverse of the Sample Correlation Matrix Estimate $\hat{\hat{\mathbf{R}}}_D[n]$

The matrix inversion lemma applied to (34) gives

$$\hat{\hat{\mathbf{R}}}_D^{-1}[n] = \tilde{\mathbf{R}}^{-1} - \left(|\alpha[n-D]|^2 I_{1,2}^{(D)} + \sigma_0^2\left(1-I_{1,2}^{(D)}\right)\right) \cdot \gamma \cdot \frac{\tilde{\mathbf{R}}^{-1}\mathbf{d}_0\mathbf{d}_0^H\tilde{\mathbf{R}}^{-1}}{\gamma+\left(|\alpha[n-D]|^2 I_{1,2}^{(D)} + \sigma_0^2\left(1-I_{1,2}^{(D)}\right)\right)}. \quad (79)$$

The inner product of the channel response with respect to the inverse of the correlation matrix can be reduced to a simple form.

$$\mathbf{c}_0^H[n-D]\hat{\hat{\mathbf{R}}}_D^{-1}[n]\mathbf{c}_0[n-D] = \frac{|\alpha|[n-D]|^2}{\gamma+\sigma_0^2\left(1-I_{1,2}^{(D)}\right)+|\alpha[n-D]|^2 I_{1,2}^{(D)}}. \quad (80)$$

APPENDIX B

It is informative to consider the SNR generated by the optimal Wiener combiner. In the context of a time-varying system, this provides the time-varying SNR that would result at the output of a Wiener combiner with perfect tracking capabilities.

The Wiener estimator of $x_0[n]$ is given by

$$\hat{x}_0[n] = \mathbf{c}_0[n]\mathbf{R}^{-1}[n]\mathbf{u}[n]. \quad (81)$$

The signal power at the output (conditioned on the channel) is

$$E_C\left(\left|\mathbf{c}_0^H[n]\mathbf{R}^{-1}[n]\mathbf{c}_0[n]x_0[n]\right|^2\right) = \left(\mathbf{c}_0^H[n]\mathbf{R}^{-1}[n]\mathbf{c}_0[n]\right)^2. \quad (82)$$

The total power of $\hat{x}_0[n]$ is

$$E_C(|\hat{x}_0[n]|^2) = \mathbf{c}_0^H[n]\mathbf{R}^{-1}[n]\mathbf{c}_0[n]. \quad (83)$$

Subtracting the signal power from the total power gives the noise power, and the time-varying SNR is

$$\Psi[n] = \frac{\mathbf{c}_0^H[n]\mathbf{R}^{-1}[n]\mathbf{c}_0[n]}{1-\mathbf{c}_0^H[n]\mathbf{R}^{-1}[n]\mathbf{c}_0[n]}. \quad (84)$$

Plugging in the results of (77) and simplifying gives

$$\Psi[n] = \frac{|\alpha[n]|^2}{\gamma}. \quad (85)$$

The SNR is proportional to the fading channel gain; therefore, the bit-error-rate performance with perfect channel tracking can be obtained by simply using the common equations for fading [2]. This has been used to provide the "perfect tracking" bit error rates of Fig. 6, with the approximation of the interferer signals as Gaussian. It is well known that this approximation holds well in DS-CDMA systems for low SNRs, but performance at higher SNRs can be better than indicated with this approximation because the tails of the binomial distribution are not as long as those of the Gaussian distribution.

APPENDIX C
PROPERTIES OF THE AR2 PROCESS

The AR2 process of interest has poles that form a conjugate pair at p and p^*, where $p = r\exp(j\theta)$, $0 \le \theta \le \pi$, excited by a white Gaussian process. The generating filter under consideration will be normalized to give an output power unchanged from the power of the white input process.

The autocorrelation function of such an AR2 process with unit power input can be found in [11]. With

$$\psi \equiv \theta - \frac{\pi}{2} - \text{angle}(1-p^2) \quad (86)$$

$$B \equiv \sin(\theta)\cdot(1-r^2)\cdot|1-p^2| \quad (87)$$

and with the process normalized to obtain a unit output power, the resulting autocorrelation function is

$$\rho[n] = \frac{r^{|n|}}{|\cos(\psi)|}\cos(|n|\theta+\psi) \quad (88)$$

and the PSD is

$$P(z)|_{|p|<|z|<|1/p|} = \frac{B}{|\cos(\psi)|} \cdot \frac{1}{(1-pz^{-1})(1-p^*z^{-1})(1-pz)(1-p^*z)}. \quad (89)$$

The power normalized two-pole filter applied to the white excitation is then

$$H_{\text{AR2}}(z)|_{|p|<|z|} = \sqrt{\frac{B}{\cos(\psi)}}\cdot\frac{1}{(1-pz^{-1})(1-p^*z^{-1})}. \quad (90)$$

The squared autocorrelation is required for (32). This is given by

$$\rho^2[n] = \frac{r^{2|n|}}{1+\cos(2\psi)}(1+\cos(2|n|\theta+2\psi)). \quad (91)$$

ACKNOWLEDGMENT

The authors would like to thank Dr. J. Proakis for his assistance and comments.

REFERENCES

[1] L. Godara, "Applications of antenna arrays to mobile communications, part I: Performance improvement, feasibility, and system considerations," *Proc. IEEE*, vol. 85, pp. 1031–1060, July 1997.

[2] J. G. Proakis, *Digital Communications*, 3rd ed. New York: McGraw-Hill, 1995.

[3] L. Godara, "Applications of antenna arrays to mobile communications, part II: Beam forming and direction of arrival considerations," *Proc. IEEE*, vol. 85, pp. 1195–1245, Aug. 1997.

[4] B. Widrow, P. E. Mantey, L. J. Griffiths, and B. B. Goode, "Adaptive antenna systems," *Proc. IEEE*, vol. 55, pp. 2143–2159, Dec. 1967.

[5] L. W. Brooks and I. S. Reed, "Equivalence of the likelihood ratio processor, the maximum signal-to-noise ratio filter, and the Wiener filter," *IEEE Trans. Aerosp. Electron. Syst.*, vol. AES-8, pp. 690–692, Sept. 1972.

[6] A. Weiss and B. Friedlander, "Fading effects on antenna arrays in cellular communications," *IEEE Trans. Signal Processing*, vol. 45, pp. 1109–1117, May 1997.
[7] H. Gao, P. Smith, and M. Clark, "Theoretical reliability of MMSE linear diversity combining in rayleigh-fading additive interference channels," *IEEE Trans. Commun.*, vol. 46, pp. 666–672, May 1998.
[8] J. Miller and S. Miller, "Smart antenna adaptive performance in the presence of imperfect power control, multipath and shadow fading," in *Conference Rec. IEEE Global Telecomm. Conf.*, vol. 1, Nov. 1997, pp. 384–388.
[9] J. Winters, "Signal acquisition and tracking with adaptive arrays in the digital mobile radio system IS-54 with flat fading," *IEEE Trans. Veh. Technol.*, vol. 42, pp. 377–384, Nov. 1993.
[10] W. Xu, M. Honig, J. Zeidler, and L. Milstein, "Subspace adaptive filtering techniques for multi-sensor DS-CDMA interference suppression," in *Conf. Rec. Thirty-Second Asilomar Conf. Signals, Syst., Comput.*, vol. 1, Nov. 1998, pp. 551–555.
[11] S. Haykin, *Adaptive Filter Theory*, 3rd ed. Upper Saddle River, NJ: Prentice-Hall, 1996.
[12] O. Macchi and N. J. Bershad, "Adaptive recovery of a chirped sinusoid in noise, 1. Performance of the RLS algorithm," *IEEE Trans. Acoust., Speech, Signal Processing*, vol. 39, pp. 583–594, Mar. 1991.
[13] P. C. Wei, J. R. Zeidler, and W. H. Ku, "Adaptive recovery of a chirped signal using the RLS algorithm," *IEEE Trans. Signal Processing*, vol. 45, pp. 969–976, Feb. 1997.
[14] S. Haykin, A. Sayed, J. Zeidler, P. Yee, and P. Wei, "Adaptive tracking of linear time-variant systems by extended RLS algorithms," *IEEE Trans. Signal Processing*, vol. 45, pp. 1118–1128, May 1997.
[15] N. J. Bershad, S. McLaughlin, and C. F. N. Cowan, "Performance comparison of RLS and LMS algorithms for tracking a first order Markov communications channel," in *Proc. IEEE Int. Symp. Circuits Syst.*, vol. 1, 1990, pp. 266–270.
[16] E. Eleftheriou and D. D. Falconer, "Tracking properties and steady state performance of RLS adaptive filter algorithms," *IEEE Trans. Acoust., Speech, Signal Processing*, vol. ASSP-34, pp. 1097–1110, Oct. 1986.
[17] E. Eweda and O. Macchi, "Tracking error bounds of adaptive nonstationary filtering," *Automatica*, vol. 21, no. 3, pp. 293–302, May 1985.
[18] B. Toplis and S. Paupathy, "Tracking improvements in fast RLS algorithms using a variable forgetting factor," *IEEE Trans, Acoust., Speech, Signal Processing*, vol. 36, pp. 206–227, Feb. 1988.
[19] J. Lin, J. Proakis, and F. Ling, "Optimal tracking of time varying channels: A frequency domain approach for known and new algorithms," *IEEE Trans. Select. Areas Commun.*, vol. 13, pp. 141–153, Jan. 1995.
[20] M. Niedzwiecki, "On tracking characteristics of weighted least squares estimators applied to nonstationary system identification," *IEEE Trans. Automat. Contr.*, vol. 33, pp. 96–98, Jan. 1988.
[21] R. Ertel, P. Cardieri, K. Sowerby, T. Rappaport, and J. Reed, "Overview of spatial channel models for antenna array communication systems," *IEEE Pers. Commun. Mag.*, vol. 5, pp. 10–22, Feb. 1998.
[22] W. C. Jakes, *Microwave Mobile Communications*. New York: Wiley, 1974.
[23] I. S. Gradshteyn and I. M. Ryzhik, *Table of Integrals, Series, and Products*, 5th ed., Academic, London, U.K., 1994.

Brian C. Banister received the B.S. and M.S. degrees in electrical engineering from the University of California at San Diego (UCSD), La Jolla, in 1993 and 1999, respectively. He is currently pursuing the Ph.D. degree with the Department of Electrical and Computer Engineering at UCSD, with research focusing on the application of multiple antenna arrays to communications and signal processing problems.

He has also been with the LSI Logic Wireless Design Center, San Diego, since 1996, where he has worked on baseband modem design and research for cellular communications systems.

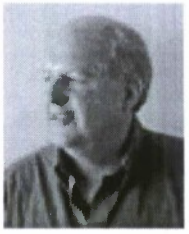

James R. Zeidler (M'76–SM'84–F94) has been a scientist at the Space and Naval Warfare Systems Center, San Diego, CA since 1974. He has also been an Adjunct Professor with the Electrical and Computer Engineering Department at the University of California at San Diego, La Jolla, since 1988. His current research interests are in adaptive signal processing, communications signal processing, and wireless communication networks.

Dr. Zeidler was an Associate Editor of the IEEE TRANSACTIONS ON SIGNAL PROCESSING from 1991 to 1994. He was co-recipient of the award for best unclassified paper at the IEEE Military Communications Conference in 1995 and received the Lauritsen–Bennet Award for achievement in science in 2000 and the Navy Meritorious Civilian Service Award in 1991.